JOURNAL OF AGRICULTURAL AND FOOD CHEMISTRY

pubs.acs.org/JAFC Article

Dietary Supplementation of Apple Phlorizin Attenuates the Redox State Related to Gut Microbiota Homeostasis in C57BL/6J Mice Fed with a High-Fat Diet

Dong Liu, Yanglin Ji, Yatu Guo, Hui Wang, Zijian Wu, Heyu Li, and Hao Wang*

Cite This: *J. Agric. Food Chem.* 2021, 69, 198−211 Read Online

ACCESS | Metrics & More | Article Recommendations | Supporting Information

ABSTRACT: We explored the effects of dietary supplementation with phlorizin on redox state-related gut microbiota homeostasis in an obesity mouse model. Mice (C57BL/6J) were grouped as follows for 12 weeks: normal chow diet group (NCD), high-fat and cholesterol diet group (HFD), and treatment groups fed with HFD along with three levels of phlorizin. Phlorizin alleviated the hyperlipidemia and redox status and increased the total ccal SCFA content (1.88 ± 0.25 mg/g). Additionally, phlorizin regulated gene expression related to lipid metabolism, redox status, and cecum barrier and rebuilt gut microbiota homeostasis. After interference by antibiotics, the total phloretin content in the feces was decreased about 4-fold, and most of the health-promoting effects were abolished, indicating that phlorizin might be susceptible to microbial biotransformation and that microecology is indispensable for maintaining the redox state capacities of phlorizin. Phlorizin treatment could be an advantageous option for improving HFD-related obesity and redox states related to gut microbiota homeostasis.

KEYWORDS: *phlorizin, gut microbiota, redox state, short-chain fatty acids, antibiotics interference*

1. INTRODUCTION

Metabolic disorders related to obesity are accompanied by high levels of reactive oxygen species (ROS) inflammation and gut dysbiosis, which is recognized as a danger of cardiovascular disease and other whole-body health factors.[1] Numerous medications are available to deal with obesity. However, these synthetic medications can have serious side-effects, such as reduction in body immunity and other disorders.[2] Adopting natural phytochemicals with few adverse side effects compared to these drugs is a novel and effective method for the amelioration of obesity and its accompanying inflammatory and oxidative stress conditions.

Obesity is related to a functional deficiency of the nuclear factor erythroid-2-related factor 2 (Nrf2), which is a vital regulator of the endogenous inducible defense systems.[3] Nrf2 is situated in the cytoplasm and is seized by Kelch-like ECH-associated protein 1 (Keap1) and ruined by the ubiquitin/proteasome system.[4] Keap1 can sense redox modifications and then separate from Nrf2, resulting in *de novo* Nrf2 accumulation and translocation to the nucleus to promote the transcription of several antioxidative or phase 2 detoxifying enzymes and related proteins, such as glutathione peroxidase (GSH-PX), catalase (CAT), and superoxide dismutase (SOD).[5] The excessive ROS in obesity could induce deficient Nrf2 translocation from the cytoplasm to the nucleus, leading to oxidative stress. Moreover, nuclear factor kappa-B (NF-κB), a redox-sensitive transcription factor, regulates the expression of proinflammatory cytokines and chemokines.[6] Oxidative stress and inflammation are indispensable, as each causes and intensifies the other, and the redox status can regulate the function of several inflammatory proteins and affect inflammatory signaling by recruiting and activating leukocytes and resident cells.[5]

Phlorizin (a phloretin 2′-glucoside) is found in the bark of apple trees and has been used in medicine because of its extensive bioactivity. Many studies have demonstrated that administration of phlorizin attenuates high-fat diet (HFD)-induced development of obesity, type 2 diabetes, hepatic steatosis, and atherosclerosis.[7] Our previous studies verified that phlorizin possesses antioxidative activity that can decrease the malondialdehyde (MDA) content, increase SOD gene expression and activity in hamsters fed with a HFD,[8] extend life span, and ameliorate the age-related decline of the locomotor function by serving as an Nrf2 activator.[9] However, less than 1% of phlorizin can be detected as a prototype in plasma, while most reaches the large intestine and undergoes a sequence of fermentation by the microbiota in systematic circulation.[10] Moreover, intestinal bacteria have been found to produce short-chain fatty acids (SCFAs) and to exert a vital role in β-glucosidase and lactase-phlorizin hydrolase (LPH) activity, including the ability to transform phlorizin to phloretin and glucose by mediating the occurrence of deglycosylation, supplying energy to cells, and enriching the medium for bacterial growth with the release of glucose.[11,12] There was no trace of intact phlorizin detected in the plasma of rats fed with a phlorizin meal in a previous study.[10] Moreover, phloretin is more effective than phlorizin at suppressing inflammation and promoting

Received: October 8, 2020
Revised: December 8, 2020
Accepted: December 9, 2020
Published: December 22, 2020

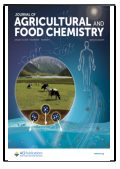

https://dx.doi.org/10.1021/acs.jafc.0c06426
J. Agric. Food Chem. 2021, 69, 198−211

lipolysis *in vitro*.[13] Similarly, Chang et al. found that in LPS-stimulated RAW264.7 cells, phloretin could suppress the inflammatory response but phlorizin could not.[14]

Therefore, based on previous findings, we hypothesized that supplementing with phlorizin would affect the redox status and modulate the Nrf2 function and related anti-inflammatory activity by maintaining gut microecology homeostasis. In order to examine our hypotheses, we inspected the hypolipidemic, antioxidant, and antiinflammation functional effects of phlorizin related to cecal SCFA levels, intestinal barrier function, and composition of gut microbiota. Moreover, an antibiotic interference experiment was used to evaluate whether the effects of phlorizin in HFD-fed mice were still significant when healthy gut microecology was demolished by antibiotics. Molecular docking was also used to identify whether phlorizin or phloretin was the more potent inhibitor of Keap1. To the best of our knowledge, this study is the first to examine the effects of phlorizin in the maintenance of a redox state based on gut microbiota homeostasis in rodents.

2. MATERIALS AND METHODS

2.1. Materials and Chemicals. Apple phlorizin and phloretin (purity > 98%) were supplied by the Binhai Jianfeng Natural Product R&D Co., Ltd. (Binhai, China). Vitamin mix and mineral mix were purchased from Harlan Laboratories Ltd (Harlan, IN). Casein was produced by Kerui Dairy Products Development Co, Ltd (Gannan, China). Other ingredients, such as lard, corn starch, sucrose, and gelatin, were acquired from the Gold Ingot farmer's market (Binhai, China). Formic acid and acetonitrile were purchased from Sigma-Aldrich (St Louis, MO). Other reagents were of analytical grade and obtained from Northern Chemical Reagent Co., Ltd. (Tianjin, China).

2.2. Animals and Diets. Male C57BL6/J mice were purchased from the Vital River Laboratory (Beijing, China). Six week-old mice were housed under controlled temperature (21−25 °C) and humidity (45−55%) conditions, with *ad libitum* access to food and sterile water under a 12 h light/dark cycle. Animal experiments were permitted by the Ethical Committee for the Experimental Use of Animals of TUST (approval no.: 20180416A) and followed the standards for care of laboratory animals outlined in the NIH Guide for the Care and Use of Laboratory Animals. Prior to the experiments, the mice were allowed to acclimatize to the animal facility environment and fed with a normal chow diet (NCD) for 7 days.

In animal study 1, mice were divided into five groups [n = 12 for 1−4th group and n = 30 for 5th (HF-PH) group] for 12 weeks and administered as follows: the NCD and HFD groups received sterile water, and HFD received phlorizin at 10 (low), 30 (middle), and 60 (high) mg/kg body weight (BW) by oral gavage daily (HF-PL, HF-PM, and HF-PH). The ingredients and composition of the diets are listed in Table 1.

Gut bacteria have been found to exert a vital role in β-glucosidase and LPH activity and have the ability to transform phlorizin to phloretin and glucose.[11,12] In previous studies, antibiotics have been shown to interfere with long-term gut microbiota dysbiosis.[15] Neomycin and ampicillin (NA) were used because they are broad-spectrum antibiotics, which are scarcely absorbed and target the microbiota of Gram-positive and Gram-negative bacteria without systemic effects.[16] In animal study 2, mice were grouped into the HFD + NA group (n = 12) and HFD + NA + PH group (n = 30) and treated with a cocktail of antibiotics (0.5 mg/mL neomycin and 1 mg/mL ampicillin) in drinking water and fed with a HFD with the presence or absence of phlorizin by oral gavage daily (high dose, 60 mg/kg BW.) for 12 weeks.

During the last week of administration, the HF-PH (n = 18) and HFD + NA + PH (n = 18) groups were transferred into a metabolism cage equipped with excretion collectors. To analyze the phlorizin/phloretin content at 1, 2, 3, 6, 12, and 24 h after oral administration, fecal and urine samples were collected on the penultimate day, and serum samples (three mice were sampled at a time) were collected on the next day. After collection of excretion and serum, the rest of the mice (n = 12 per group) was fasted for 12 h with free access to water and were then humanely exsanguinated from the retro-orbital sinus. Organ and tissues were frozen and fixed for molecular biological and micropathological analysis.

Table 1. Ingredients and Composition of Different Diets

	NCD	HFD
Ingredient (g/kg)		
casein	212	212
sucrose	50.0	50.0
vitamin mix	15.0	15.0
D−L methionine	1.00	1.00
mineral mix	35.0	35.0
gelatin	10.0	10.0
lard	50.0	200
cholesterol	0	1.00
corn starch	627	476
Composition		
protein (g/kg)	200	200
TEP[a] (%)	19.8	16.7
fat (g/kg)	50.0	200
TEF[b] (%)	11.2	37.7
carbohydrate (g/kg)	696	545
TEC[c] (%)	69.0	45.6
total energy(kJ/kg)	**16,877**	**19,998**

[a]TEP, total energy from protein. [b]TEF, total energy from fat. [c]TEC, total energy from carbohydrate.

2.3. Dosage Information. The design of the phlorizin dosages in three treatment groups was based on the literature[17] and on our preliminary experiments. The dosage of 10, 30, and 60 mg/kg BW per day for mice was equivalent to adult human consumption of 0.81, 2.43, and 4.86 mg/kg BW per day based on the body surface area.[18]

2.4. HPLC Assay. The concentrations of phlorizin and phloretin in the feces, urine, and serum were determined using HPLC (SHIMADZU, Japan) equipped with a C18 column (4.6 × 250 mm, 5 μm) for chromatographic separation. The mobile phase consisted of two phases monitored at 280 nm: A is water/formic acid (99:1, v/v), and B is acetonitrile (100%). The injection volume was 10 μL, and a 30 °C-column temperature and 1.0 mL/min flow rate were used. Samples were dissolved in phase A and filtered through a 0.22 μm membrane filter. The elution conditions were as follows: 0−15 min, 5−15% B; 15−21 min, 15−28% B; 21−22 min, 28−40% B, 22−24 min, 40−60% B; 24−27 min, 60−5% B; and 27−40 min, 5% B.

2.5. Serum, Hepatic, and Intestinal Parameter Analyses. The blood samples were collected in 1.5 mL tubes containing heparin sodium for anticoagulation and centrifuged at 3500g for 15 min at 4 °C. Following the manufacturer's instructions, triglyceride (TG), total cholesterol (TC), high-density lipoprotein cholesterol (HDL-C), lipopolysaccharides (LPS), tumor necrosis factor-alpha (TNF-α), and interleukin-6 (IL-6) content were determined by commercial reagent kits obtained from the Nanjing Jiancheng Biological Technology Institute (Nanjing, China). Non-high-density lipoprotein cholesterol (non-HDL-C) was computed using the following formula: non-HDL-C = TC − HDL-C.

The serum, liver, and cecal activity of CAT, GSH-PX, SOD, MDA content, and total antioxidant capacity (T-AOC) were detected using assay kits (Nanjing Jiancheng Biological Technology Institute, China). Chloroform−methanol (2:1) solution was used to extract hepatic TG and TC in accordance with Folch et al.[19] and then assayed using assay kits.

2.6. Histological Analysis. After being fixed in 10% (v/v) formalin solution, epididymal white adipose tissues (EWATs) and hepatic and intestinal tissues were embedded in paraffin, cut into 4 μm sections, and stained with hematoxylin−eosin (H&E) for morphological observation. Slides were photographed using an optical microscope (Olympus,

https://dx.doi.org/10.1021/acs.jafc.0c06426
J. Agric. Food Chem. 2021, 69, 198−211

Table 2. Primer Sequences Used for Real-Time PCR Analysis

target gene/bacterium	forward primer	reverse primer
GAPDH	GCATCTTCTTGTGCAGTGCC	TACGGCCAAATCCGTTCACA
AMPKα	GGACTTACTTGTTGGATTTCCG	CCTTTGGCAAGATCGATAGTTG
PPARγ	GGAATTAGATGACAGTGACTTG	TCTTCTGGAGCACCTTGG
FASN	TCGTCTATACCACTGCTTACTAC	CACACCACCTGAACCTGAG
SREBP-1c	CTGCTAGCTAGATGACCCTGC	TCTGGCTTTGATCCCGGAAG
PPARα	CACGAAGCCTACCTGAAG	GTGGAAGAATCGGACCTC
CPT1α	AACAACGGCAGAGCAGAG	ACACCACATAGAGGCAGAAG
ACC1	GGCAGCAGTTACACCACATAC	TCATTACCTCAATCTCAGCATAGC
Nrf2	TTCAGCAGCATCCTCTCC	GGTCACAGCCTTCAATAGTC
CAT	CAGGTGCGGACATTCTAC	GCGTTCTTAGGCTTCTCAG
GSH-PX	AGAACTGTCAGAACGAGGAG	GGGTCATCATAAGGGTAGGG
Cu, Zn-SOD	GAACCAGTTGTGTTGTCAGG	CCGTCCTTTCCAGCAGTC
Mn-SOD	GACCTGCCTTACGACTATG	GAAGAGCGACCTGAGTTG
TLR-4	TTCACCTCTGCCTTCACTAC	GACACTACCACAATAACCTTCC
NF-κB	AGTGGGAATTTCCAGCCAGG	GCGTGCAGGTGGATGTTTTT
TNF-α	TTGTCTACTCCCAGGTTCTCTTC	AATCGGCTGACGGTGTGG
IL-6	CCCCAATTTCCAATGCTCTCC	CGCACTAGGTTTGCCGAGTA
Mucin2	GAAGCCAGATCCCGAAACCA	GAATCGGTAGACATCGCCGT
JAM	ATTTGGCTGGAACTACCGCA	GAGTACTTGCGCTCAGGAGG
Occludin	GAGGCTATGGCTATGGCTATGG	AGGAAGCGATGAAGCAGAAGG
Bifidobacterium	GGGTGGTAATGCCGGATG	CCACCGTTACACCGGGAA
Lactobacillus	AGCAGTAGGGAATCTTCCA	CACCGCTACACATGGAG

Japan). All images were measured using ImageJ software (National Institutes of Health, USA).

2.7. Gene Expression Analysis. A real-time polymerase chain reaction (PCR) system (iCycler, Bio-Rad, CA) was used to determine the gene expression of the liver and cecal tissues as described in our previous study.[20] The quantification of target gene expression was performed by the $2^{-\Delta\Delta C_T}$ method. To identify the abundance of *Bifidobacterium* and *Lactobacillus*, sequences were amplified from cecal bacteria gDNA and then cloned into the vector pMD19-T (Takara Bio) to construct the standard plasmid. The forward and reverse primers of *Bifidobacterium*, *Lactobacillus*,[21,22] and others are shown in Table 2.

2.8. Cecal SCFA Analysis. The cecal SCFA (acetic, propionic, and butyric acid) analysis was performed described in our previous study.[23] Briefly, cecal SCFAs were quantified using GC equipped with a flame ionization detector and HP-INNO Wax chromatographic column (30 m × 320 μm × 0.25 μm) (Agilent 7890A, USA).

2.9. Cecal DNA Extraction and High-Throughput Sequencing. Cecal contents were gathered and stored at −80 °C, genomic DNA was extracted, and 16S rRNA gene V4 regions with primers were amplified, using 515F and 806R. High throughput sequencing was generated on the Illumina HiSeq2500 platform. High-quality reads were obtained by Uparse and identified to the same OTUs (≥97% similarity). Representative sequences from each OTU were assigned to their corresponding taxonomy based on the GreenGenes database. Alpha and beta diversities were examined by QIIME and shown in R software.

2.10. *In Silico* Assay. The crystallographic structure of the mouse Keap1 protein without the N-terminal region of the Nrf2 transcription factor was obtained from the PDB protein data bank (http://www.rcsb.org/, ID: 2DYH). In this study, we investigated how phlorizin and phloretin interacted with Keap1. The structures of phlorizin (CAS: 60-81-1) and phloretin (CAS: 60-82-2) were downloaded from ChemicalBook (https://www.chemicalbook.com) and treated as ligands. The methods of active docking site selection and ligand/receptor preparation were as previously described.[9] Discover Studio 3.5 (DS3.5 Accelrys, US) was employed for molecular modeling of the compounds with Keap1. The one with the lowest energy in complex with the receptor was identified. The conformation with the lowest energy of conformation was deemed as the most appropriate.

2.11. Statistical Analysis. Data analyses were performed using GraphPad Prism software and shown as mean ± standard deviation (SD). The difference between two groups was analyzed using a the two-tailed Student's *t*-test. Comparisons between more than two groups were conducted using one-way analysis of variance followed by Tukey's *post hoc* test. The *P*-values of less than 0.05 ($P < 0.05$) were considered significant. The correlation and significance of body weight, TC, TG, T-AOC, cecal SCFAs, and so forth, and relative abundance of bacteria were examined by Pearson's correlation (SPSS 20, USA).

3. RESULTS

3.1. Growth Parameters and Profiles of the Serum and Liver. After phlorizin treatment, in comparison with the HFD group, the body weight of the HF-PH group was reduced by 16.70% ($P < 0.05$, Figure 1A). There was no significant difference in food or energy intake among HFD-based groups ($P > 0.05$, Figure 1B). At the same time, the elevated levels of serum TG, TC, and non-HDL-C under HFD feeding were reduced by HF-PH treatment ($P < 0.05$, Figure 1C). Additionally, phlorizin treatment reversed the increase in liver TC and TG levels caused by HFD ($P < 0.05$, Figure 1D). These results indicate that phlorizin may weaken the phenotype induced by the HFD.

3.2. Oxidative Stress in the Serum, Liver, and Cecum. Obesity is accompanied by a high level of oxidative stress, which has been extensively studied in rodents, while antioxidant enzymes exert defense against oxidative stress. In this study, T-AOC, CAT, SOD, and GSH-PX activity and MDA content in the serum, liver, and cecum were used to assess the redox state. As demonstrated in Figure 2, the HFD group showed increased oxidative stress compared to the NCD group and elevated content of MDA, as well as reduced activity of T-AOC, CAT, SOD, and GSH-PX. However, supplementation with phlorizin restored obesity-related oxidative stress in the serum, liver, and cecum in the HF-PH group ($P < 0.05$, Figure 2), although there was no difference of CAT in the liver, SOD in the serum, liver, and cecum, GSH-PX in the serum and liver, and MDA in the serum between the HF-PL group and HFD group ($P > 0.05$).

3.3. Inflammation Cytokine Levels in the Serum. Various proinflammatory cytokines, such as TNF-α and IL-6, which are secreted by hypertrophic adipocytes, were robustly

https://dx.doi.org/10.1021/acs.jafc.0c06426
J. Agric. Food Chem. 2021, 69, 198−211

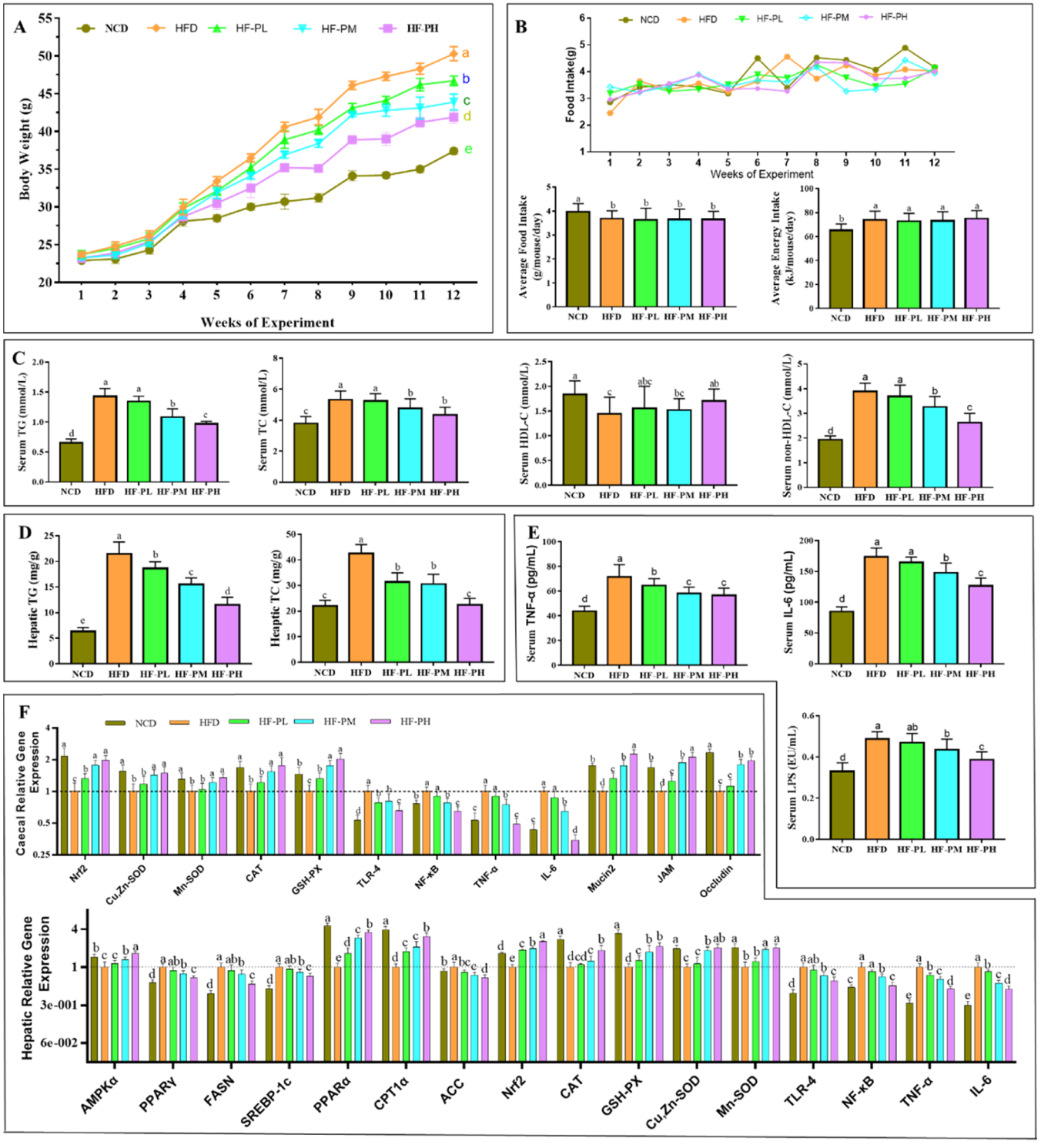

Figure 1. Effects of phlorizin on body weight (A); food and energy intake (B); serum lipid levels of TG, TC, HDL-C, and non-HDL-C (C); hepatic TG and TC (D); serum endotoxin and inflammatory cytokine levels of TNF-α, IL-6, and LPS (E); mRNA expression of lipids metabolism, oxidative stress, and inflammation and intestinal barrier integrity of the liver and caecum (F). Values are expressed as mean ± SD of 12 mice per group and which in each bar with different letters indicate significantly differences ($P < 0.05$).

amplified during the development of obesity.[24] In this study, phlorizin supplementation reduced the raised serum levels of TNF-α and IL-6 compared to those in the HFD group ($P < 0.05$, Figure 1E).

Furthermore, the increased number of enterotoxins, such as LPS entering the circulatory system in obesity, can result in high penetrability of the intestinal barrier.[25] As shown in Figure 1E, the increased LPS content induced by HFD in serum was significantly reversed after phlorizin intervention in HF-PH and HF-PM groups ($P < 0.05$), but no difference was observed in the HF-PL group ($P > 0.05$).

3.4. Histopathological Analysis. To identify the protective effects of phlorizin administration, histopathological analysis of the EWAT, hepatic and intestinal tissues in obesity

https://dx.doi.org/10.1021/acs.jafc.0c06426
J. Agric. Food Chem. 2021, 69, 198−211

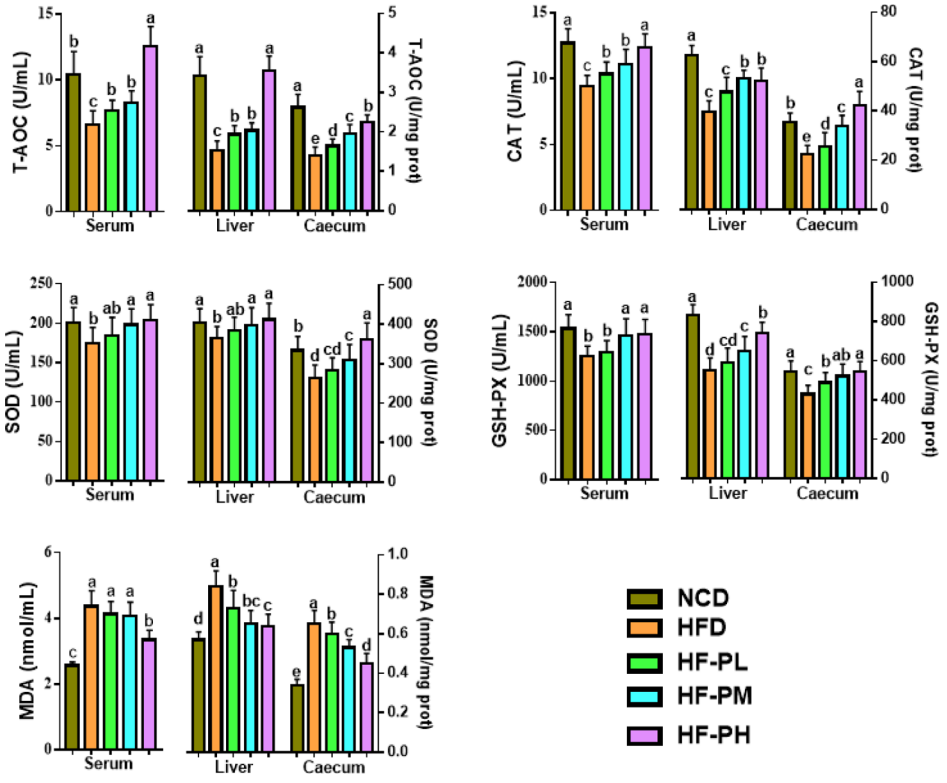

Figure 2. Effects of phlorizin on oxidative stress associated indicators of the serum, liver and cecum. Values are expressed as mean ± SD of 12 mice per group and which in each bar with different letters indicate significantly differences ($P < 0.05$).

mice was inspected by H&E staining (Figure 3A). The average size of EWAT adipocytes in the HFD group was larger than that in the HF-PH group ($P < 0.05$, Figure 3B). The liver cells in the NCD group had a typical hepatic cell shape with a well-preserved cytoplasm, a clear nucleus, and a central vein, while the HFD group had sickly hepatic steatosis and the infiltration of inflammatory cells. Phlorizin supplementation recovered HFD-induced liver damage and preserved liver parenchyma with fewer cytoplasmic lipid vacuoles.

Compared to the NCD group, the villus height in the ileum and the area percentage of colonic goblet cells per crypt of the HFD group were significantly reduced ($P < 0.05$, Figure 3B). Phlorizin administration significantly increased ileum villus heights. At the same time, infiltration of inflammatory cells, ulceration, and epithelial damage were also detected in the cecum and colon of mice fed with HFD. These data indicate that the intestinal barrier function was destroyed by HFD, while phlorizin administration improved the mechanical barrier function of the intestine.

3.5. Cecal SCFAs. The HFD reduced the total SCFA content compared to that of the NCD group ($P < 0.05$, Table 3), while phlorizin administration increased the SCFA levels, in particular, HF-PH increased the propionic acid content by 3.33-fold and butyric acid content by 1.81-fold ($P < 0.05$, Table 3).

3.6. Gene Expression in the Liver and Cecum. The mRNA expression of lipid metabolism-related genes in the liver was evaluated by PCR analysis. The mRNA expression of the α-subunit of adenosine 5′-monophosphate-activated protein kinase (AMPKα), a fundamental regulator of energy balance, was increased in the HF-PH groups compared with that in the HFD group ($P < 0.05$, Figure 1F). The expression of fatty acid synthesis-related genes, including peroxisome proliferator-activated receptor γ (PPARγ), fatty acid synthase (FASN), sterol regulatory element-binding protein 1c (SREBP-1c), and acetyl-coenzyme A carboxylase alpha (ACC1), was significantly decreased in the HF-PH group compared to the HFD group ($P < 0.05$). Meanwhile, the mRNA expression of genes related to β-oxidation of fatty acids, such as peroxisome proliferator-activated receptor α (PPARα) and carnitine palmitoyltransferase 1α (CPT1α), was increased in the HF-PH group ($P < 0.05$).

Furthermore, phlorizin (HF-PH group) treatment improved the expression of genes encoding Nrf2, GSH-PX, Mn-SOD, Cu, Zn-SOD, and CAT relative to the HFD group both in the liver and cecum ($P < 0.05$, Figure 1F). The HFD-induced mice displayed significantly higher gene expression of proinflammatory cytokines (TNF-α and IL-6) in the liver and cecal tissue compared to the NCD. The high dose of phlorizin significantly decreased proinflammatory cytokine gene expression in the liver and cecum ($P < 0.05$, Figure 1F). Moreover, the cecal and hepatic relative mRNA expressions of toll-like receptor 4 (TLR-4) and NF-κB were also reduced by phlorizin supplementation in HFD-induced obesity mice. These results suggest that phlorizin could alleviate HFD-induced inflammation and oxidative stress, at least in part, *via* the NF-κB and Nrf2 pathways.

A major protective mechanism is to use the tight-junction protein to maintain the integrity of the gut epithelial cells and multilayered mucus structures to keep a safe distance between gut epithelial cells and microbiota.[26] The HF-PH group showed a positive effect on the mRNA expression of tight-junction and mucus genes, such as junctional adhesion molecule (JAM), occludin, and mucin2, in the cecum ($P < 0.05$, Figure 1F).

3.7. Composition of Gut Microbiota. The composition of gut microbiota differs between obese and lean people. An investigation of diversity indexes indicated that phlorizin intervention improves the ACE, Chao1, and Shannon indexes,

https://dx.doi.org/10.1021/acs.jafc.0c06426
J. Agric. Food Chem. 2021, 69, 198−211

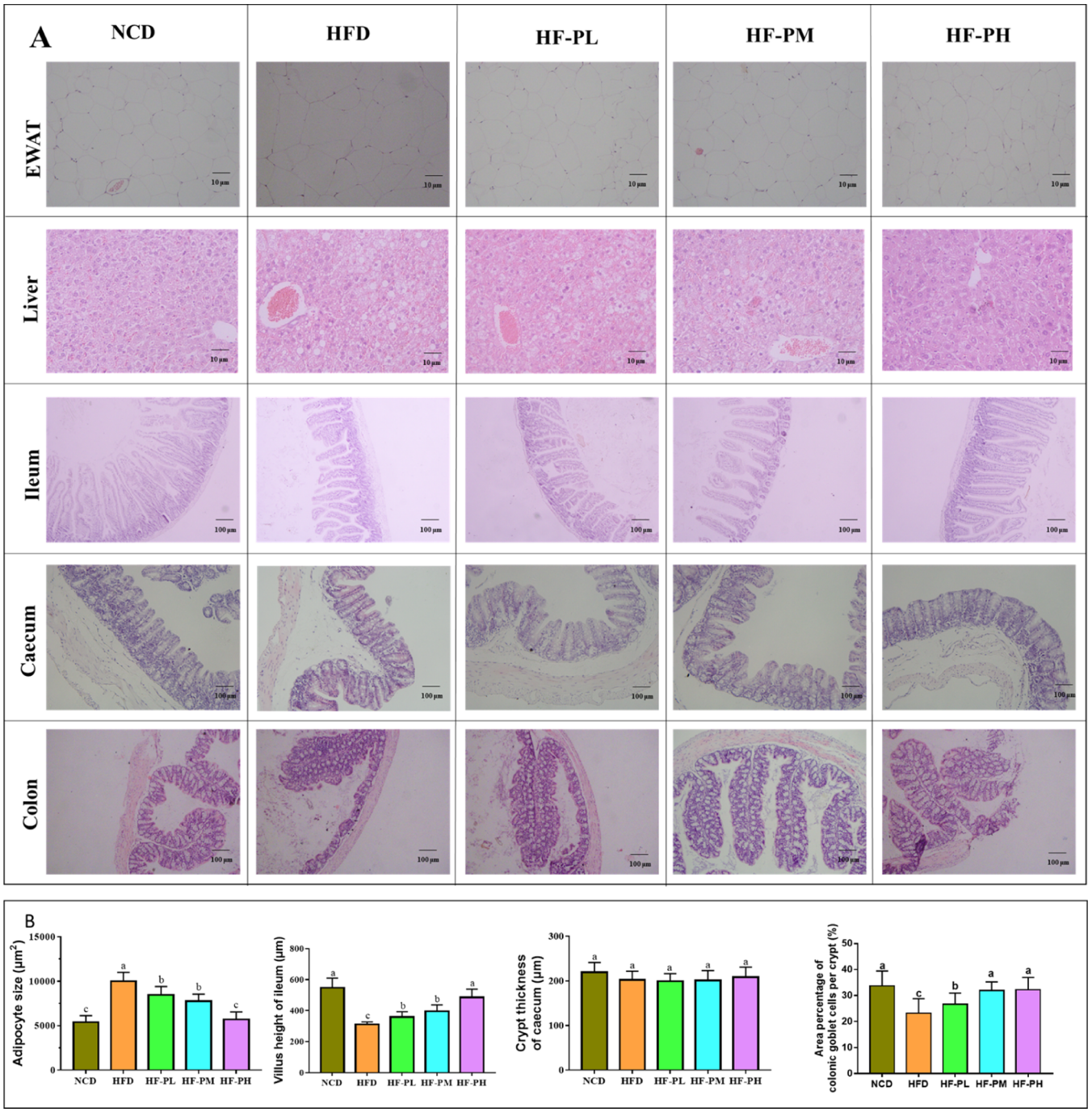

Figure 3. Effects of phlorizin treatment on HFD-induced histopathologic alterations in the EWAT, liver and intestine (ileum, cecum, and colon) examined by H&E staining (A). Effects of phlorizin treatment on the adipocyte size of EWAT, villus height of ileum, crypt thickness of cecum, and the area percentage of colonic goblet cells per crypt (B). Values are expressed as mean ± SD of 12 mice per group and which in each bar with different letters indicate significantly differences ($P < 0.05$).

Table 3. Effects of Phlorizin on Cecal SCFA Concentration[a]

parameters	NCD	HFD	HF-PL	HF-PM	HF-PH
			Cecal SCFAs (mg/g)		
acetic acid	0.86 ± 0.06 a	0.21 ± 0.02 e	0.34 ± 0.04 d	0.41 ± 0.05 c	0.68 ± 0.08 b
propanoic acid	0.52 ± 0.06 b	0.18 ± 0.02 e	0.30 ± 0.04 d	0.37 ± 0.05 c	0.60 ± 0.07 a
butyric acid	0.67 ± 0.05 a	0.32 ± 0.05 e	0.38 ± 0.04 d	0.45 ± 0.06 c	0.58 ± 0.07 b
total	**2.03±0.25 a**	**0.72±0.12 d**	**1.01±0.14 c**	**1.25±0.21 b**	**1.88±0.25 a**

[a]Values are expressed as mean ± SD of 12 mice per group and which in each line with different letters indicate significantly differences ($P < 0.05$).

https://dx.doi.org/10.1021/acs.jafc.0c06426
J. Agric. Food Chem. 2021, 69, 198−211

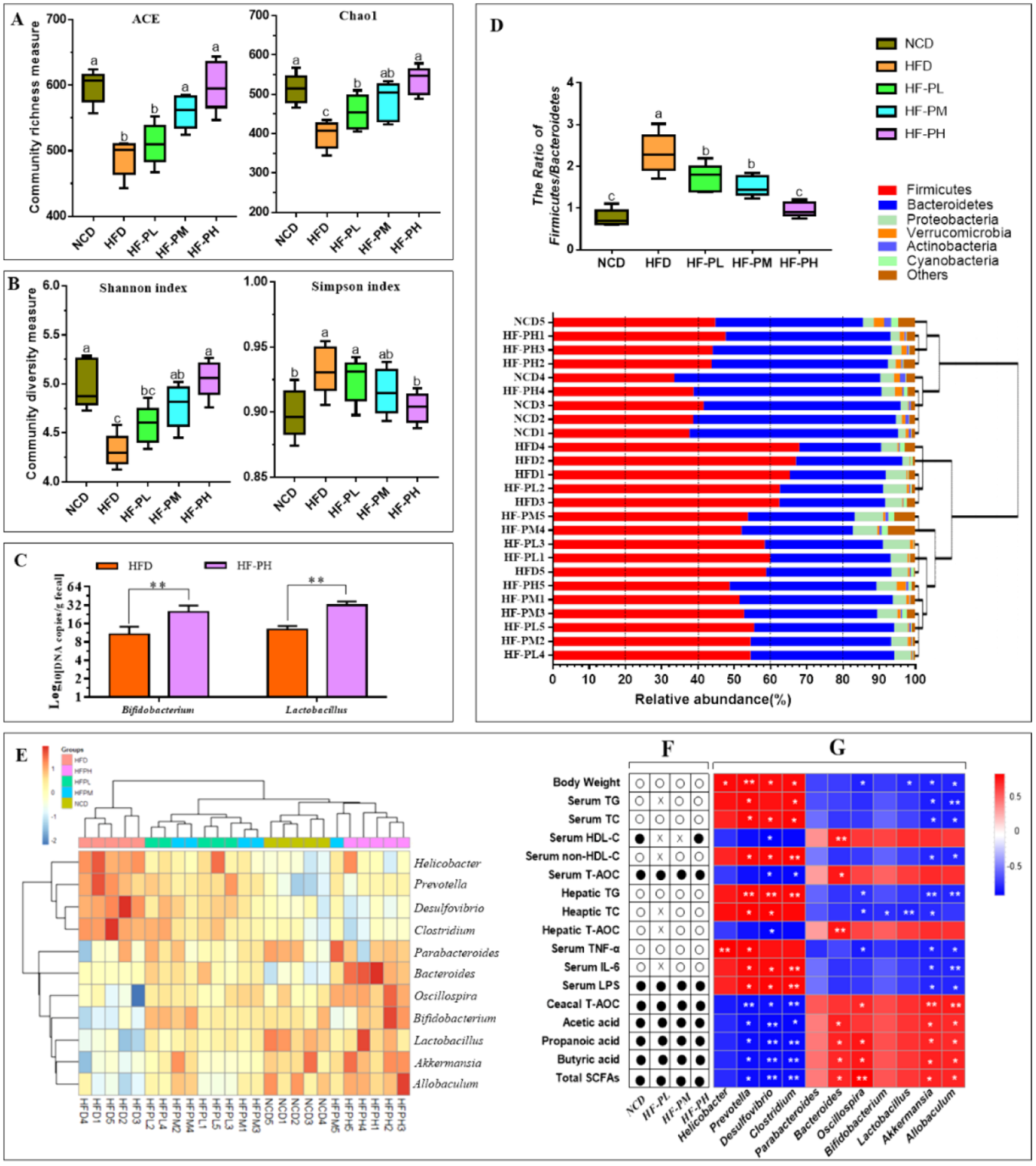

Figure 4. Richness and diversity of gut microbiota accessed by ACE, Chao1, Shannon index, and Simpson index (A,B). Effect of phlorizin treatment on cecal bacterial (*Bifidobacterium* and *Lactobacillus*) contents measured by PCR (C); the ratio of Firmicutes/Bacteroidetes, relative abundances of gut microbiota at the phylum level (D) and at the genus level (E). Values are expressed as mean ± SD of 12 mice per group and which in each bar with different letters indicate significantly differences ($P < 0.05$, A–D). The circular (○), (●), and (×) signified the lower, higher, and no significant levels in other groups when compared with the HFD group, respectively ($P < 0.05$, F). The results of Pearson's correlation between the relative abundance of gut microbiota and other levels (body weight, oxidative stress, inflammation, and cecal SCFAs concentration) (G, color of squares from blue to red represents *P*-value of Pearson's correlation, * ($P < 0.05$) and ** ($P < 0.01$) represent significant and extremely significant correlation).

while reducing the Simpson index in the HF-PH group at the species level ($P < 0.05$, Figure 4A,B). Taxonomic profiling analysis was used to inspect the variation of the gut microbiota after phlorizin administration at the phylum level. A clear separation between the NCD and HF-PH and HFD, HF-PL, and HF-PM groups is shown in Figure 4D, which indicates that

https://dx.doi.org/10.1021/acs.jafc.0c06426
J. Agric. Food Chem. 2021, 69, 198−211

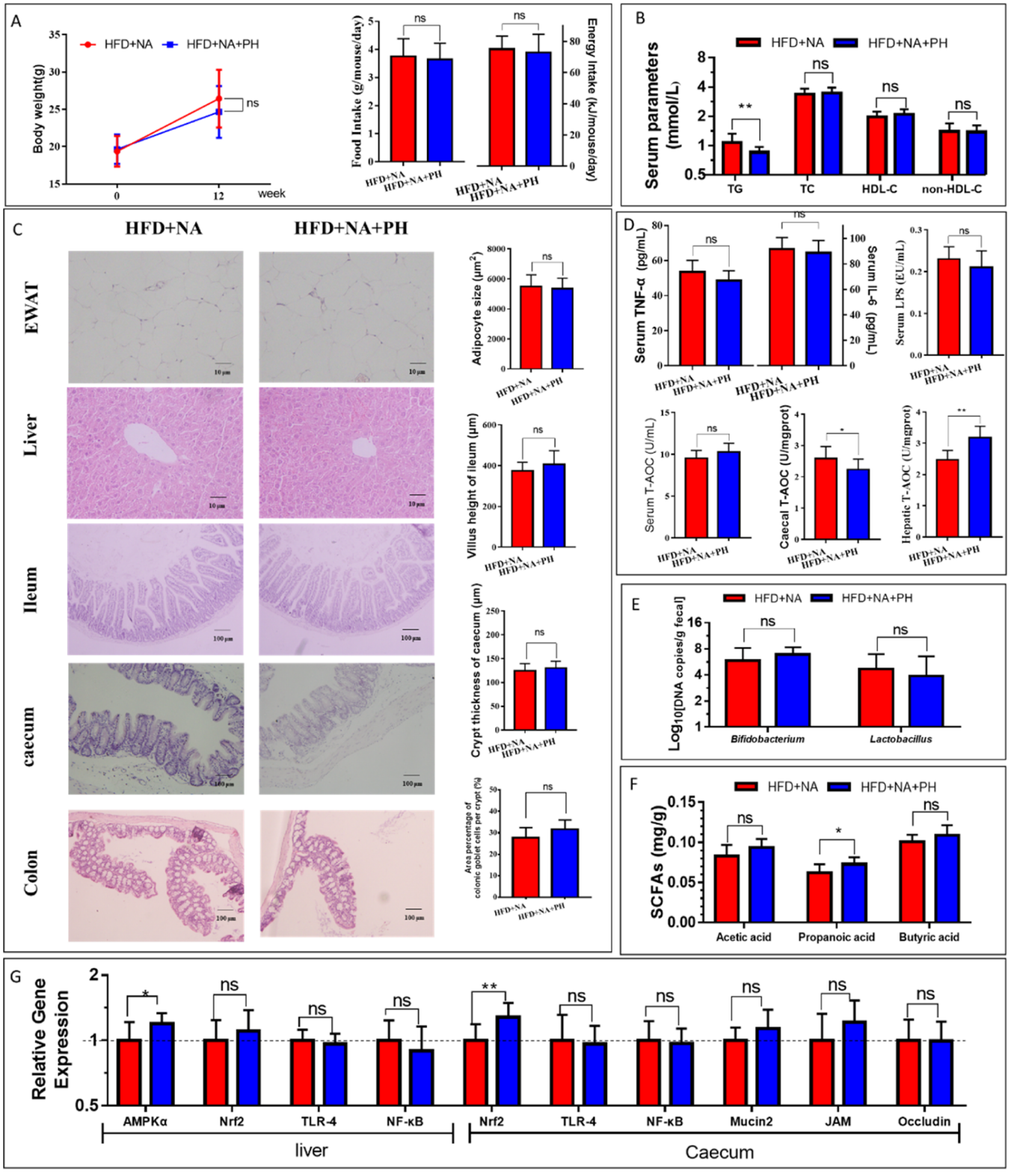

Figure 5. Gut microbiota relates effects of phlorizin treatment in antibiotics interfered experiment. Effects of phlorizin on body weight, food, and energy intake (A); serum parameters (B,D); morphology of the EWAT, liver, specific intestine (C); cecal bacterial (*Bifidobacterium* and *Lactobacillus*) contents (E); cecal SCFAs contents (F); mRNA expression of lipids metabolism, oxidative stress, and inflammation and intestinal integrity of the liver and cecum (G). Values are expressed as mean ± SD with no significant (ns, $P > 0.05$), significant (*, $P < 0.05$), and extremely significant (**, $P < 0.01$) differences in each bar of 12 mice per group.

phlorizin intervention could shift the gut microbiota composition to that of the NCD group.

In addition, Firmicutes/Bacteroidetes are positively associated with obesity.[27] As shown in Figure 4D, the Firmicutes/Bacteroidetes in the HF-PH group were reduced by 56.22% in

https://dx.doi.org/10.1021/acs.jafc.0c06426
J. Agric. Food Chem. 2021, 69, 198−211

Table 4. Excretion and Serum Phlorizin and Phloretin in HF-PH and HFD + NA + PH Groups[a]

group		HF-PH group				HFD + NA + PH group			
		phlorizin		phloretin		phlorizin		phloretin	
sample/mouse	interval (h)	nmol/h	(%)	nmol/h	(%)	nmol/h	(%)	nmol/h	(%)
urine	0−1	14.3 ± 1.12 a	(0.35 ± 0.03)	0.62 ± 0.04 b	(0.02 ± 0.01)	17.0 ± 0.21	(0.42 ± 0.01)	--	(--)
	1−2	21.5 ± 0.39 a	(0.52 ± 0.03)	2.19 ± 0.04 b	(0.06 ± 0.01)	24.5 ± 0.27 a	(0.60 ± 0.01)	0.29 ± 0.07 b	(--)
	2−3	33.5 ± 0.14 a	(0.81 ± 0.01)	3.43 ± 0.07 b	(0.09 ± 0.01)	27.3 ± 0.18 a	(0.70 ± 0.01)	0.55 ± 0.11 b	(--)
	3−6	20.6 ± 0.18 a	(1.50 ± 0.06)	0.95 ± 0.07 b	(0.07 ± 0.01)	22.1 ± 0.14	(1.71 ± 0.01)	--	(--)
	6−12	0.27 ± 0.02	(0.04 ± 0.01)	--	(--)	4.97 ± 0.05	(0.77 ± 0.01)	--	(--)
	12−24	0.16 ± 0.02	(0.05 ± 0.01)	--	(--)	0.18 ± 0.02	(0.06 ± 0.01)	--	(--)
feces	0−1	29.3 ± 0.99 b	(0.71 ± 0.03)	47.8 ± 0.18 a	(1.23 ± 0.01)	66.2 ± 0.55 a	(1.70 ± 0.01)	16.7 ± 0.40 b	(0.43 ± 0.01)
	1−2	34.4 ± 0.80 b	(0.83 ± 0.02)	54.7 ± 0.62 a	(1.41 ± 0.02)	112 ± 0.41 a	(2.78 ± 0.01)	24.2 ± 0.69 b	(0.62 ± 0.02)
	2−3	38.0 ± 0.25 b	(0.92 ± 0.01)	220 ± 1.24 a	(5.67 ± 0.03)	157 ± 0.48 a	(4.06 ± 0.01)	37.9 ± 0.33 b	(0.98 ± 0.01)
	3−6	29.6 ± 0.09 b	(2.18 ± 0.01)	76.6 ± 0.33 a	(5.91 ± 0.03)	121 ± 0.25 a	(9.16 ± 0.02)	31.6 ± 0.47 b	(2.44 ± 0.04)
	6−12	14.3 ± 0.11 b	(2.11 ± 0.02)	39.0 ± 0.07 a	(6.03 ± 0.01)	42.9 ± 0.27 a	(6.62 ± 0.04)	10.9 ± 0.29 b	(1.68 ± 0.05)
	12−24	3.28 ± 0.05	(1.01 ± 0.01)	--	(--)	4.67 ± 0.21	(1.34 ± 0.06)	--	(--)

group		HF-PH group		HFD + NA + PH group	
sample/mouse	interval (h)	Phlorizin (nmol/mL)	phloretin (nmol/mL)	phlorizin (nmol/mL)	phloretin (nmol/mL)
serum	0−1	0.18 ± 0.02	--	0.16 ± 0.02	--
	1−2	0.27 ± 0.05 a	0.07 ± 0.04 b	0.34 ± 0.02	--
	2−3	0.78 ± 0.05 a	0.51 ± 0.07 b	0.96 ± 0.02	--
	3−6	0.30 ± 0.02 a	0.22 ± 0.04 b	0.50 ± 0.05	--
	6−12	0.18 ± 0.02 a	0.18 ± 0.03 a	0.25 ± 0.05	--
	12−24	--	0.07 ± 0.04	--	--

[a]Proportions (%) are expressed as the mole ratio [MW phlorizin (molecular weight), 436.41; MW phloretin, 274.27]. Values are expressed as mean ± SD of 3 mice per period and which in each line with different letters indicate significant differences between phlorizin and phloretin ($P < 0.05$). "--", not detected or numbers <0.01.

comparison with the HFD group ($P < 0.05$). Further, the relative abundance of *Allobaculum*, *Akkermansia*, *Bacteroides*, *Lactobacillus*, and *Bifidobacterium* was reduced, while *Clostridium*, *Helicobacter*, *Prevotella*, and *Desulfovibrio* were increased in the HFD group compared to the NCD group at the genus level (Figure 4E). Phlorizin administration robustly inverted these alterations induced by HFD.

As shown in Figure 4F, all of the indicators related to metabolic disorder were significantly ameliorated in the HF-PH group ($P < 0.05$). Furthermore, the correlation between and significance of those indicators and the relative abundance of bacteria were examined by Pearson's correlation. As shown in Figure 4G ($P < 0.01$), *Helicobacter* was positively associated with serum TNF-α; *Prevotella* was negatively associated with cecal T-AOC and positively associated with hepatic TG and body weight; *Desulfovibrio* was negatively associated with total SCFAs, butyric acid, propanoic acid, and acetic acid and positively associated with hepatic TG; *Clostridium* was negatively associated with total SCFAs, butyric acid, propanoic acid, and cecal T-AOC and positively associated with serum LPS, serum IL-6, hepatic TG, and serum non-HDL-C; *Bacteroides* was positively associated with cecal T-AOC and serum HDL-C; *Oscillospria* was positively correlated with total SCFAs; *Lactobacillus* was negatively associated with hepatic TC; *Akkermansia* was negatively associated with hepatic TG and positively associated with cecal T-AOC; *Allobaculum* was negatively associated with serum TG, hepatic TG, and serum IL-6 but positively associated with cecal T-AOC.

3.8. Gut Microbiota Related to the Redox State. To identify whether microbiota was indispensable for maintaining a redox state under phlorizin intervention, gut dysbiosis was induced with antibiotics. During 12 weeks of NA interference, phlorizin supplementation was unable to elevate the levels of *Bifidobacterium* and *Lactobacillus*, as shown by PCR tests (Figure 5E). Consistently, cecal SCFAs were at low levels with no significant difference between the two groups aside from propanoic acid (Figure 5F).

There were no significant changes in the final body weight, food, and energy intake, serum TC, HDL-C, or non-HDL between the HFD + NA and HFD + NA + PH groups except for TG in the antibiotic-treated experiment (Figure 5A,B). Furthermore, phlorizin administration did not alter the levels of serum TNF-α, IL-6, LPS, T-AOC, or adipocyte size of the EWAT or villus height compared to the HFD + NA group (Figure 5C,F).

Additionally, in comparison with the HFD + NA group, phlorizin supplementation did not affect the gene expression of Nrf2, TLR-4, or NF-κB in the liver. Meanwhile, phlorizin supplementation did not modify the gene expression of TLR-4, NF-κB, mucin2, JAM, or occludin in the cecum (Figure 5G), while phlorizin increased the expression of AMPKα (liver, $P < 0.05$) and Nrf2 (cecum, $P < 0.01$) (Figure 5G).

3.9. Transformation of Phloretin after Antibiotic Interference in the Feces. To compare the transformation of phlorizin after antibiotic interference, excretion and serum samples were analyzed at 1, 2, 3, 6, 12, and 24 after oral administration. Figure S1 shows the chromatograms of feces, urine, and serum extracts from the HF-PH and HFD + NA + PH groups detected at 280 nm. Peak 1 (28.50 min) and peak 2 (30.50 min) were identical to the retention times of standard phlorizin and phloretin, respectively. In the HF-PH group, less than 7% (n/n, expressed as the mole ratio) of the total number was present in the form of phloretin in the urine. Meanwhile, more than 72% (n/n) of phlorizin was transformed to phloretin in the feces (Figure S1, Table 4). However, administration of antibiotics to the HFD + NA + PH group decreased by 70% ($n/$

https://dx.doi.org/10.1021/acs.jafc.0c06426
J. Agric. Food Chem. 2021, 69, 198−211

n) of phloretin proportions in the feces compared to the HF-PH group. At the same time, almost none of the phloretin detected in the urine and serum seemed to be susceptible to microbial biotransformation due to phlorizin (Figure S1, Table 4).

3.10. Binding Affinity of Phloretin and Phlorizin into Keap1 *In Silico*. Transcription factor Nrf2 and its principal negative regulator (Keap1) significantly contribute to the regulation of redox, metabolic, and protein homeostasis, as well as to inflammation.[28] Computational analysis has been used to study the effect of small inhibitory molecules on the partnership of keap1 and Nrf2.[29] A structural assessment was used to study the interactions between these two compounds and the catalytic or regulatory site of Keap1. As a result, phloretin and phlorizin were identified as direct inhibitors of the Keap1-Nrf2 interaction, as evidenced by its high binding affinity and occupancy of specific binding sites of the Klech domain (Figure S2). After docking to the active pocket, phlorizin and phloretin interacted with the peripheral residues *via* secondary bonding, such as hydrogen bonding, van der Waals, electrostatic, and hydrophobic interactions. The negative value indicated that the interaction between phlorizin, phloretin, and the receptor was in a steady state.

Phloretin has stronger hydrophobicity than phlorizin. From the aspect of binding energy, phloretin (−10.54 kcal/mol) has higher affinity than phlorizin (−8.61 kcal/mol) to Keap1, and ligand stabilization of phloretin in the hydrophobic binding pocket mainly relies on pi−pi interactions (ARG415) and hydrogen bonds (GLY367, VAL606, VAL418, and LEU365). Similarly, it has been reported that Keap1 inhibitors could interact with the ARG415 hydrophobic binding pocket.[30] Furthermore, in the structure of the Keap1−phlorizin complex, some steric hindrance was found between sugar chain atoms and the hydrophobic binding pocket. Thus, compared to phlorizin, phloretin has more ability to enhance Nrf2 activity by acting as a Keap1 inhibitor, suggesting its potential as an antioxidant.

4. DISCUSSION

There is comprehensive agreement that phytonutrients have the capacity to regulate oxidative stress, inflammation, and gut microbiota related to obesity. Phlorizin is an excellent phytonutrient and shows robust ROS-scavenging and lipid-lowering activity both *in vivo* and *in vitro*.[8,31] In the present study, we found that phlorizin supplementation effectively alleviated obesity, oxidative stress, and inflammation owing to its capability for maintaining gut microbiota homeostasis in C57BL/6J mice fed with HFD.

Epidemiological indications show that both body weight gain and lipid profile elevation are related to HFD. After 12 weeks administration, phlorizin significantly reduced body weight, serum TC, TG, and non-HDL-C content in the HF-PH group (Figure 1A−C). At the same time, it decreased hepatic TC and TG contents (Figure 1D). This is in line with an earlier finding that C57BL/6J mice treated with 20 mg/kg BW. phlorizin for 13 weeks had significantly decreased weight gain, blood lipid levels, and hyperplasia of the adipocytes.[17]

Furthermore, obesity is associated with changed mRNA expression in the liver related to lipid metabolism. AMPKα is a vital regulator of energy balance that modulates serial mRNA expression. HFD induces high expression of PPARγ and increases the transcription of target genes related to lipid *de novo* synthesis.[32] In contrast to PPARγ, PPARα regulates several genes related to β-oxidation.[33] In this study, phlorizin reduced the gene expression levels of PPARγ, SERBP-1c, FASN, and ACC1, whereas it restored the levels of AMPKα, PPARα, and CPT1α ($P < 0.05$, Figure 1F). These results were in agreement with the decrease of TG and TC levels in the liver ($P < 0.05$, Figure 1D) and the alleviation of hepatic lipid accumulation with phlorizin treatment (Figure 3A). It was also in line with previous findings that phlorizin significantly reduces hepatic lipids (TC and TG)[34] and that phloretin prevents obesity by inhibiting *de novo* lipogenesis in HFD-induced mice.[35] Nevertheless, Huang et al. found that phloretin significantly activates AMPKα in a concentration-dependent manner, while phlorizin does not significantly modulate AMPKα in mouse 3T3-L1 cells.[13] Given these different conclusions *in vivo* and *in vitro* and the fact that gut bacteria play a vital role in β-glucosidase and LPH activity with the ability to transform phlorizin to phloretin,[11,12] we presumed that gut bacteria are indispensable to the beneficial effects of phlorizin *in vivo*.

In addition, HFD can lead to the generation of fat-mediated oxidative stress, thereby shifting the cellular redox-environment to an oxidized state. We measured the activity of three antioxidant enzymes (CAT, GSH-PX, and SOD) and the content of an oxidant marker (MDA). Overall, HFD clearly decreased antioxidant capacity, leading to oxidative stress and contributing to disease pathogenesis in the liver and cecum (Figures 2 and 3). Similarly, our previous study showed that phlorizin supplementation attenuates serum and liver oxidative stress by increasing SOD, CAT, GSH-PX, and T-AOC activity and reduces the MDA content by promoting the gene expression of Nrf2 in hamsters fed with HFDs.[8] However, there is an intimate association between inflammation and redox alteration.[36] Researchers have found that a dysfunction in the Nrf2 system is related to the initiation of inflammation, which, in turn, promotes ROS production, leading to redox imbalance by triggering redox-sensitive transcription factors and signal transduction pathways, further leading to obesity and consequent metabolic aberrances.[37,38]

Metabolic syndrome related to obesity can trigger low-grade inflammation and increase proinflammatory markers (such as TNF-α and IL-6). Thus, obesity can result in dysbiosis of the intestinal redox state leading to NF-κB activation through receptor TLR-4 by the bacterial product LPS.[39] Furthermore, prolonged inflammation induced by LPS leads to export of Nrf2 out of the nucleus and prevents the binding of Nrf2-ARE.[40] Hypertrophic adipocytes also can secrete various proinflammatory cytokines such as TNF-α and IL-6. Our study examined the antienterotoxins and antiproinflammatory activity of phlorizin by reducing the content of serum LPS, TNF-α, and IL-6 (Figure 1E). We also observed that phlorizin treatment increased the mRNA expression of Nrf2, CAT, GSH-PX, Cu, Zn-SOD, and Mn-SOD levels, meanwhile decreasing TLR-4, NF-κB, TNF-α, and IL-6 mRNA expression in both the liver and cecal tissues (Figure 1F).

LPS has been shown to induce inflammation by damaging the gut barrier function.[41] A deficiency of tight and adhesive junctions between the gut epithelial cells increases the penetrability of the gut barrier, which allows more enterotoxins such as LPS to enter the circulatory system and induce inflammation and obesity.[25] Our results showed that phlorizin could enhance the gut barrier function and decrease proinflammatory levels by decreasing the LPS content. This was in agreement with a previous study showing that phlorizin from *Docynia indica* (Wall.) attenuates metabolic disorder, which is related to anti-inflammation, and intestinal barrier function by reducing serum TNF-α, IL-6, and LPS and

https://dx.doi.org/10.1021/acs.jafc.0c06426
J. Agric. Food Chem. 2021, 69, 198−211

improving the jejunum villus height.[17] Gut microbiota homeostasis is crucial for system health, but changes in microbiome composition were not involved in the aforementioned study. Therefore, an antibiotic interference experiment was further used to evaluate whether the protective effects of phlorizin *in vivo* were dependent on the transformation of phlorizin to phloretin by gut bacteria in the present study.

In metabolic disorder, disturbances in SCFA production are always accompanied by gut microbiota and barrier dysbiosis. Furthermore, SCFAs positively affect gut health by fortifying the gut barrier function, promoting mucus secretion, and regulating lipid metabolism.[27] In the present study, phlorizin restored the decrease in the cecal SCFA content, which supports a recent finding that phlorizin has an antimicrobial effect by promoting SCFA production.[39] Furthermore, butyric acid serves as a key energy source for the host colonic epithelium and increases mucus secretion,[42] which was increased by phlorizin treatment in the present study ($P < 0.05$, Table 3). As presented in Figure 3A, phlorizin has beneficial effects on the pathology of the ileum, cecum, and colon and restores the cecal gene expression of mucin2, JAM, and occludin.

Further, intestinal redox-state-related obesity may also affect microbiota composition. The increased ACE, Chao1, and Shannon and decreased Simpson indexes suggest that gut microbiota abundance and diversity were modified upon supplementation with phlorizin (Figure 4A,B). In addition, obese individuals have a higher ratio of Firmicutes/Bacteroidetes compared to lean individuals.[43] In high-throughput sequencing analysis, the ratio of Firmicutes/Bacteroidetes was improved by HFD at the phylum level, while it was normalized by administration of phlorizin ($P < 0.05$, Figure 4D). At the genus level, *Bifidobacterium* and *Lactobacillus* have the ability to increase SCFA concentration, reduce serum TC, and exert a key role in β-glucosidase and LPH activity by hydrolyzing phlorizin to phloretin, and phloretin showed antibacterial activity that was at least 10-fold higher than that of phlorizin.[12,39] In the present study, more than 72% (n/n) of phlorizin was transformed to phloretin after oral gavage (Figure 1S). Similarly, Crespy et al. evaluated the absorption and metabolism of phloretin/phlorizin in rats and indicated that the conjugated forms are detected in blood and that glucoside cleavage from the phlorizin structure must be performed before conjugation and absorption from the mucosal and serosal sides.[44]

Studies indicate that *Akkermansia* can decrease lipid aggregation, counteract metabolic endotoxemia (such as serum LPS), and strengthen epithelial integrity. It is reduced by HFD.[45,46] Moreover, gut dysbiosis and metabolic syndromes increase the abundance of *Prevotella* and *Clostridium*, which are also positively associated with chronic inflammation, inflammatory bowel disease, and pathogenic microorganisms.[47,48] Consistent with these findings, in this study, HFD-induced mice had a higher relative abundance of *Prevotella* and *Clostridium* and lower abundance of *Akkermansia* as compared to the NCD group (Figure 4E). *Akkermansia* was negatively associated with hepatic TG and positively associated with cecal T-AOC; *Prevotella* was negatively associated with cecal T-AOC and positively associated with hepatic TG and body weight; *Clostridium* was negatively associated with total SCFAs, butyric acid, propanoic acid, and cecal T-AOC and positively associated with serum LPS, serum IL-6, hepatic TG, and serum non-HDL-C ($P < 0.01$, Figure 4G). Administration of phlorizin boosted the enrichment of *Allobaculum* and *Oscillospria* (Figure 4E), which has been shown to produce SCFAs in the gut.[47] Besides producing butyrate, *Oscillospria* is also related to the low body mass index.[49] Similarly, in the present study, *Oscillospria* was negatively associated with the final body weight and hepatic TG and TC ($P < 0.05$), while it was positively correlated with the cecal T-AOC activity ($P < 0.05$) and total SCFA content ($P < 0.01$, Figure 4G). Furthermore, *Desulfovibrio* was negatively associated with total SCFAs, butyric acid, propanoic acid, and acetic acid and positively associated with hepatic TG ($P < 0.01$, Figure 4G). We found that phlorizin treatment restored the increase of *Desulfovibrio* induced by HFD (Figure 4E), which generates H_2S related to the destruction of gut epithelial cells.[50] Corresponding to the outcomes of microbiota sequencing, treatment of phlorizin boosted the relative abundance of *Lactobacillus* and *Bifidobacterium* by PCR in the HF-PH group (Figure 4C). Similarly, Mei et al. also indicated that administration of phlorizin has hypoglycemic activity by increasing SCFAs, decreasing LPS, and producing beneficial bacteria, particularly modified *Akkermansia* and *Prevotella*, in obese and type 2 diabetes (*db*/*db*) mice.[39]

Previous studies have revealed that interference with broad-spectrum antibiotics can cause long-standing gut dysbiosis in rodents. In the present study, administration of broad-spectrum antibiotics blunted the biotransformation of phlorizin to phloretin, which resulted in lower phloretin content in the feces and indicated that this biotransformation is highly susceptible to microbial degradation in the gut (Table 4, Figure S1). Similarly, Esposito et al. found that compared to anthocyanin-treated obese mice, administration of anthocyanin plus antibiotic cocktail resulted in a 16−25-fold increase in anthocyanin and a 2−4-fold decrease in phenolic acid (anthocyanin-derived metabolites) in the feces.[51]

At the same time, we adopted antibiotics to promote gut dysbiosis and verified that phlorizin did not affect the relative abundance of *Bifidobacterium* and *Lactobacillus* (Figure 5E). Furthermore, antibiotics dulled the effect of phlorizin in the final body weight, serum TC, HDL-C, non-HDL-C, TNF-α, IL-6, LPS, T-AOC, cecal SCFA content, the mRNA expression in the liver (Nrf2, TLR-4, and NF-κB), and cecum (TLR-4, NF-κB, Mucin2, JAM, and occludin), and the ability to restore the intestinal barrier function (Figure 5C). Similarly, Zeng et al. found that the metabolic protective effects, including prevention of increased body weight, serum TC, and decreased HDL-C, of PMFE (rich in polymethoxyflavones) were abolished in HFD mice treated with a cocktail of antibiotics.[52] Thus, the antibiotic treatment study offered new insights into the potential relationships between phlorizin intake and health benefits. However, antibiotic-induced gut dysbiosis mice were not germ-free, and the prebiotic effects of phlorizin were weakened but not totally lost. Furthermore, along with its prebiotic effects *in vivo*, phlorizin was also shown directly to exert antioxidant properties by its reductive structure or via the Nrf2 pathway, to lower lipid accumulation in HepG2 cells and to reduce inflammation in macrophages.[28,53] Additionally, phloretin is more effective than phlorizin at suppressing inflammation and promoting lipolysis *in vitro*.[13] Thus, in the HFD + NA + PH group, the reduction of phloretin further dulled its beneficial effects.

Generally, Nrf2 can separate from Keap1 and translocate to the nucleus to promote the transcription of several antioxidative or phase 2 detoxifying enzymes. Thus, molecular docking was used to inspect the most potential inhibitor of Keap1 (Figure S2) and showed that phloretin blocks the Nrf2 binding site of Keap1 and helps to alleviate the level of Nrf2.

https://dx.doi.org/10.1021/acs.jafc.0c06426
J. Agric. Food Chem. 2021, 69, 198−211

In conclusion, this study shows that consumption of phlorizin for 12 weeks could ameliorate HFD-induced obesity and alleviate both oxidative stress and inflammation in the serum, liver, and cecum in HFD-fed obesity mice. Meanwhile, gut microbiota sequencing studies and antibiotic interference experiment indicated that phlorizin could rebuild intestinal microecology dysbiosis caused by HFD and was indispensable for maintaining the redox state effects of phlorizin. However, the uptake of phlorizin is complex *in vivo*, and it can be assimilated and metabolized into phloretin in the gut. The crosstalk between phlorizin, phloretin, and intestinal microecology is vital for host health, which should be examined in terms of different omics in future studies.

■ ASSOCIATED CONTENT

Supporting Information

The Supporting Information is available free of charge at https://pubs.acs.org/doi/10.1021/acs.jafc.0c06426.

HPLC chromatograms and 3D and 2D illustration (PDF)

■ AUTHOR INFORMATION

Corresponding Author

Hao Wang − *State Key Laboratory of Food Nutrition and Safety, Tianjin University of Science & Technology, Tianjin 300457, China;* orcid.org/0000-0001-5975-506X; Phone: +86-22-60912431; Email: wanghao@tust.edu.cn; Fax: +86-22-60912431

Authors

Dong Liu − *State Key Laboratory of Food Nutrition and Safety, Tianjin University of Science & Technology, Tianjin 300457, China; Jiangsu Key Laboratory of Preventive and Translational Medicine for Geriatric Disease, Department of Nutrition and Food Hygiene, School of Public Health, Medical College of Soochow University, Suzhou 215123, China;* orcid.org/0000-0003-2043-5346

Yanglin Ji − *State Key Laboratory of Food Nutrition and Safety, Tianjin University of Science & Technology, Tianjin 300457, China*

Yatu Guo − *Tianjin Key Lab of Ophthalmology and Visual Science, Tianjin Eye Hospital, Tianjin Eye Institute, Tianjin 300384, China*

Hui Wang − *Tianjin Municipal Public Security Hospital, Tianjin 300042, China*

Zijian Wu − *College of Biotechnology and Food Science, Tianjin University of Commerce, Tianjin 30014, China*

Heyu Li − *Tianjin Ubasio Biotechnology Group Co., Ltd, Tianjin 300457, China*

Complete contact information is available at: https://pubs.acs.org/10.1021/acs.jafc.0c06426

Author Contributions

D.L. and Y.J. contributed equally to this work. H.W. conceived and supervised the study; D.L. designed the experiments; D.L. and Y.J. performed the experiments; D.L. wrote the manuscript; Y.G. and H.W. corrected the article; Z.W. and H.L. revised the manuscript. All authors reviewed the results and approved the final version of the manuscript.

Funding

This work was supported by the fund of the National Natural Science Foundation of China [no. 81300791], the Natural Science Foundation of Tianjin [nos. 14JCQNJC10500 and 18JCYBJC26500], the Tianjin science and technology project [17KPHDSF00120], and the "Novel technology and relative mechanism of agricultural products processing and storage" Tianjin innovation team of university [TD13-5087].

Notes

The authors declare no competing financial interest.

■ ABBREVIATIONS

ACC1, acetyl-Coenzyme A carboxylase alpha; **AMPKα**, α subunit of adenosine 5'-monophosphate-activated protein kinase; **BW**, body weight; **CAT**, catalase; **CPT1α**, carnitine palmitoyltransferase 1α; **EWAT**, epididymal white adipose tissue; **FASN**, fatty acid synthase; **GSH-PX**, glutathione peroxidase; **HDL-C**, high-density lipoprotein cholesterol; **HFD**, high-fat diet; **HF-PH**, high-fat diet supplemented with high dose of phlorizin; **HF-PL**, high-fat diet supplemented with low dose of phlorizin; **HF-PM**, high-fat diet supplemented with middle dose of phlorizin; **IL-6**, interleukin-6; **JAM**, junctional adhesion molecule; **Keap1**, Kelch-like ECH-associated protein 1; **LPH**, lactase-phlorizin hydrolase; **LPS**, lipopolysaccharides; **MDA**, malondialdehyde; **MW**, molecular weight; **NA**, neomycin and ampicillin; **NCD**, normal chow diet; **NF-κB**, nuclear factor kappa-B; **non-HDL-C**, non-high-density lipoprotein cholesterol; **Nrf2**, nuclear factor erythroid-2-related factor 2; **PCR**, polymerase chain reaction; **PPAR**, α/γ, peroxisome proliferator-activated receptor α/γ; **ROS**, reactive oxygen species; **SCFAs**, short-chain fatty acids; **SD**, standard deviation; **SOD**, superoxide dismutase; **SREBP-1c**, sterol regulatory element-binding protein 1c; **T-AOC**, total antioxidant capacity; **TC**, total cholesterol; **TG**, triglyceride; **TLR-4**, toll-like receptor 4; **TNF-α**, tumor necrosis factor-alpha; **TUST**, Tianjin University of Science and Technology

■ REFERENCES

(1) Qiao, Y.; Sun, J.; Ding, Y.; Le, G.; Shi, Y. Alterations of the gut microbiota in high-fat diet mice is strongly linked to oxidative stress. *Appl. Microbiol. Biotechnol.* **2013**, *97*, 1689−1697.

(2) Powell, T. M.; Khera, A. Therapeutic Approaches to Obesity. *Curr. Treat. Options Cardiovasc. Med.* **2010**, *12*, 381−395.

(3) He, H.-J.; Wang, G. Y.; Gao, Y.; Ling, W. H.; Yu, Z. W.; Jin, T. R. Curcumin attenuates Nrf2 signaling defect, oxidative stress in muscle and glucose intolerance in high fat diet-fed mice. *World J. Diabetes* **2012**, *3*, 94−104.

(4) Zhang, D. D. Mechanistic studies of the Nrf2-Keap1 signaling pathway. *Drug Metab. Rev.* **2006**, *38*, 769−789.

(5) Ruiz, S.; Pergola, P. E.; Zager, R. A.; Vaziri, N. D. Targeting the transcription factor Nrf2 to ameliorate oxidative stress and inflammation in chronic kidney disease. *Kidney Int.* **2013**, *83*, 1029−1041.

(6) Cachofeiro, V.; Goicochea, M.; de Vinuesa, S. G.; Oubiña, P.; Lahera, V.; Luño, J. Oxidative stress and inflammation, a link between chronic kidney disease and cardiovascular disease. *Kidney Int. Suppl.* **2008**, *74*, S4−S9.

(7) Cremonini, E.; Daveri, E.; Mastaloudis, A.; Adamo, A. M.; Mills, D.; Kalanetra, K.; Hester, S. N.; Wood, S. M.; Fraga, C. G.; Oteiza, P. I. Anthocyanins protect the gastrointestinal tract from high fat diet-induced alterations in redox signaling, barrier integrity and dysbiosis. *Redox Biol.* **2019**, *26*, 101269.

(8) Wang, H.; Sun, Z.; Rehman, R.-U.; Shen, T.; Riaz, S.; Li, X.; Hua, E.; Zhao, J. Apple phlorizin supplementation attenuates oxidative stress in hamsters fed a high-fat diet. *J. Food Biochem.* **2018**, *42*, No. e12445.

(9) Wang, H.; Sun, Z.; Liu, D.; Li, X.; Rehman, R. U.; Wang, H.; Wu, Z. Apple phlorizin attenuates oxidative stress in Drosophila melanogaster. *J. Food Biochem.* **2019**, *43*, No. e12744.

(10) Crespy, V.; Aprikian, O.; Morand, C.; Besson, C.; Manach, C.; Demigné, C.; Rémésy, C. Bioavailability of phloretin and phloridzin in rats. *J. Nutr.* **2001**, *131*, 3227−3230.
(11) Faria, A.; Fernandes, I.; Norberto, S.; Mateus, N.; Calhau, C. Interplay between Anthocyanins and Gut Microbiota. *J. Agric. Food Chem.* **2014**, *62*, 6898−6902.
(12) Park, Y. H.; Kim, J. G.; Shin, Y. W.; Kim, H. S.; Kim, Y.-J.; Chun, T.; Kim, S. H.; Whang, K. Y. Effects of *Lactobacillus acidophilus* 43121 and a Mixture of *Lactobacillus casei* and *Bifidobacterium longum* on the Serum Cholesterol Level and Fecal Sterol Excretion in Hypercholesterolemia-Induced Pigs. *Biosci. Biotechnol. Biochem.* **2014**, *72*, 595−600.
(13) Huang, W.-C.; Chang, W.-T.; Wu, S.-J.; Xu, P.-Y.; Ting, N.-C.; Liou, C.-J. Phloretin and phlorizin promote lipolysis and inhibit inflammation in mouse 3T3-L1 cells and in macrophage-adipocyte co-cultures. *Mol. Nutr. Food Res.* **2013**, *57*, 1803−1813.
(14) Chang, W.-T.; Huang, W.-C.; Liou, C.-J. Evaluation of the anti-inflammatory effects of phloretin and phlorizin in lipopolysaccharide-stimulated mouse macrophages. *Food Chem.* **2012**, *134*, 972−979.
(15) Cani, P. D.; Bibiloni, R.; Knauf, C.; Waget, A.; Neyrinck, A. M.; Delzenne, N. M.; Burcelin, R. Changes in gut microbiota control metabolic endotoxemia-induced inflammation in high-fat diet-induced obesity and diabetes in mice. *Diabetes* **2008**, *57*, 1470−1481.
(16) Ferrier, L.; Bérard, F.; Debrauwer, L.; Chabo, C.; Langella, P.; Buéno, L.; Fioramonti, J. Impairment of the Intestinal Barrier by Ethanol Involves Enteric Microflora and Mast Cell Activation in Rodents. *Am. J. Pathol.* **2006**, *168*, 1148−1154.
(17) Zhang, X.-y.; Yi, K.; Chen, J.; Li, R.-p.; Xie, J.; Jin, Y.; Mei, X.-r.; Li, Y.-j.; Liu, G.; Wang, Z.-g. Purified Phlorizin from *DocynIa Indica* (Wall.) Decne by HSCCC, Compared with Whole Extract, Phlorizin and Non-Phlorizin Fragment Ameliorate Obesity, Insulin Resistance, and Improves Intestinal Barrier Function in High-Fat-Diet-Fed Mice. *Molecules* **2018**, *23*, 2701.
(18) Reagan-Shaw, S.; Nihal, M.; Ahmad, N. Dose translation from animal to human studies revisited. *FASEB J.* **2008**, *22*, 659−661.
(19) Folch, J.; Lees, M.; Sloane Stanley, G. H. A simple method for the isolation and purification of total lipides from animal tissues. *J. Biol. Chem.* **1957**, *226*, 497−509.
(20) Liu, D.; Ji, Y.; Zhao, J.; Wang, H.; Guo, Y.; Wang, H. Black rice (*Oryza sativa* L.) reduces obesity and improves lipid metabolism in C57BL/6J mice fed a high-fat diet. *J. Funct. Foods* **2020**, *64*, 103605.
(21) Rinttila, T.; Kassinen, A.; Malinen, E.; Krogius, L.; Palva, A. Development of an extensive set of 16S rDNA-targeted primers for quantification of pathogenic and indigenous bacteria in faecal samples by real-time PCR. *J. Appl. Microbiol.* **2004**, *97*, 1166−1177.
(22) Langendijk, P. S.; Schut, F.; Jansen, G. J.; Raangs, G. C.; Kamphuis, G. R.; Wilkinson, M. H.; Welling, G. W. Quantitative fluorescence in situ hybridization of Bifidobacterium spp. with genus-specific 16S rRNA-targeted probes and its application in fecal samples. *Appl. Environ. Microbiol.* **1995**, *61*, 3069−3075.
(23) Li, X.; Zhang, Z.; Cheng, J.; Diao, C.; Yan, Y.; Liu, D.; Wang, H.; Zheng, F. Dietary supplementation of soybean-derived sterols regulates cholesterol metabolism and intestinal microbiota in hamsters. *J. Funct. Foods* **2019**, *59*, 242−250.
(24) Marginean, C. O.; Melit, L. E.; Hutanu, A.; Ghiga, D. V.; Sasaran, M. O. The adipokines and inflammatory status in the era of pediatric obesity. *Cytokine* **2020**, *126*, 154925.
(25) Zhou, L.; Wang, X.; Shao, L.; Yang, Y.; Shang, W.; Yuan, G.; Jiang, B.; Li, F.; Tang, J.; Jing, H.; Chen, M. Berberine acutely inhibits insulin secretion from beta-cells through 3′,5′-cyclic adenosine 5′-monophosphate signaling pathway. *Endocrinology* **2008**, *149*, 4510−4518.
(26) Liang, Y.; Zhan, J.; Liu, D.; Luo, M.; Han, J.; Liu, X.; Liu, C.; Cheng, Z.; Zhou, Z.; Wang, P. Organophosphorus pesticide chlorpyrifos intake promotes obesity and insulin resistance through impacting gut and gut microbiota. *Microbiome* **2019**, *7*, 19.
(27) Jamar, G.; Estadella, D.; Pisani, L. P. Contribution of anthocyanin-rich foods in obesity control through gut microbiota interactions. *Biofactors* **2017**, *43*, 507−516.
(28) Akmal, A.; Javaid, A.; Hussain, R.; Kanwal, A.; Zubair, M.; Ashfaq, U. A. Screening of phytochemicals against KEAP1-NRF2 interaction to reactivate NRF2 Functioning: Pharmacoinformatics based approach. *Pak. J. Pharm. Sci.* **2019**, *33*, 2823−2828.
(29) Lu, M.-C.; Ji, J.-A.; Jiang, Z.-Y.; You, Q.-D. The Keap1-Nrf2-ARE Pathway As a Potential Preventive and Therapeutic Target: An Update. *Med. Res. Rev.* **2016**, *36*, 924−963.
(30) Jiang, Z.-Y.; Lu, M.-C.; Xu, L. L.; Yang, T.-T.; Xi, M.-Y.; Xu, X.-L.; Guo, X.-K.; Zhang, X.-J.; You, Q.-D.; Sun, H.-P. Discovery of potent Keap1-Nrf2 protein-protein interaction inhibitor based on molecular binding determinants analysis. *J. Med. Chem.* **2014**, *57*, 2736−2745.
(31) Wang, H.; Cheng, J.; Wang, H.; Wang, M.; Zhao, J.; Wu, Z. Protective effect of apple phlorizin on hydrogen peroxide-induced cell damage in HepG2 cells. *J. Food Biochem.* **2019**, *43*, No. e13052.
(32) Gao, J.; Song, J.; Du, M.; Mao, X. Bovine α-lactalbumin hydrolysates (α-LAH) attenuate high-fat diet induced nonalcoholic fatty liver disease by modulating hepatic lipid metabolism in C57BL/6J mice. *J. Funct. Foods* **2019**, *54*, 254−262.
(33) Goto, T. A review of the studies on food-derived factors which regulate energy metabolism via the modulation of lipid-sensing nuclear receptors. *Biosci., Biotechnol., Biochem.* **2019**, *83*, 579−588.
(34) Tian, Y.; Gao, L.; Guo, Y.; Xu, Y. Short-term phlorizin treatment attenuates adipose tissue inflammation without alerting obesity in high-fat diet fed mice. *J. Food Biochem.* **2017**, *41*, No. e12407.
(35) Alsanea, S.; Gao, M.; Liu, D. Phloretin Prevents High-Fat Diet-Induced Obesity and Improves Metabolic Homeostasis. *AAPS J.* **2017**, *19*, 797−805.
(36) Pedruzzi, L. M.; Cardozo, L. F. M. F.; Daleprane, J. B.; Stockler-Pinto, M. B.; Monteiro, E. B.; Leite, M., Jr.; Vaziri, N. D.; Mafra, D. Systemic inflammation and oxidative stress in hemodialysis patients are associated with down-regulation of Nrf2. *J. Nephrol.* **2015**, *28*, 495−501.
(37) Ren, L.; Zhan, P.; Wang, Q.; Wang, C.; Liu, Y.; Yu, Z.; Zhang, S. Curcumin upregulates the Nrf2 system by repressing inflammatory signaling-mediated Keap1 expression in insulin-resistant conditions. *Biochem. Biophys. Res. Commun.* **2019**, *514*, 691−698.
(38) Blaser, H.; Dostert, C.; Mak, T. W.; Brenner, D. TNF and ROS Crosstalk in Inflammation. *Trends Cell Biol.* **2016**, *26*, 249−261.
(39) Mei, X.; Zhang, X.; Wang, Z.; Gao, Z.; Liu, G.; Hu, H.; Zou, L.; Li, X. Insulin Sensitivity-Enhancing Activity of Phlorizin Is Associated with Lipopolysaccharide Decrease and Gut Microbiota Changes in Obese and Type 2 Diabetes (*db/db*) Mice. *J. Agric. Food Chem.* **2016**, *64*, 7502−7511.
(40) Sandberg, M.; Patil, J.; D'Angelo, B.; Weber, S. G.; Mallard, C. NRF2-regulation in brain health and disease: Implication of cerebral inflammation. *Neuropharmacology* **2014**, *79*, 298−306.
(41) Cani, P. D.; Possemiers, S.; Van de Wiele, T.; Guiot, Y.; Everard, A.; Rottier, O.; Geurts, L.; Naslain, D.; Neyrinck, A.; Lambert, D. M.; Muccioli, G. G.; Delzenne, N. M. Changes in gut microbiota control inflammation in obese mice through a mechanism involving GLP-2-driven improvement of gut permeability. *Gut* **2009**, *58*, 1091−1103.
(42) Zheng, L.; Kelly, C. J.; Battista, K. D.; Schaefer, R.; Lanis, J. M.; Alexeev, E. E.; Wang, R. X.; Onyiah, J. C.; Kominsky, D. J.; Colgan, S. P. Microbial-Derived Butyrate Promotes Epithelial Barrier Function through IL-10 Receptor−Dependent Repression of Claudin-2. *J. Immunol.* **2017**, *199*, 2976−2984.
(43) Turnbaugh, P. J.; Ley, R. E.; Mahowald, M. A.; Magrini, V.; Mardis, E. R.; Gordon, J. I. An obesity-associated gut microbiome with increased capacity for energy harvest. *Nature* **2006**, *444*, 1027−1031.
(44) Crespy, V.; Morand, C.; Besson, C.; Manach, C.; Démigné, C.; Rémésy, C. Comparison of the Intestinal Absorption of Quercetin, Phloretin and Their Glucosides in Rats. *J. Nutr.* **2001**, *131*, 2109−2114.
(45) Everard, A.; Belzer, C.; Geurts, L.; Ouwerkerk, J. P.; Druart, C.; Bindels, L. B.; Guiot, Y.; Derrien, M.; Muccioli, G. G.; Delzenne, N. M.; de Vos, W. M.; Cani, P. D. Cross-talk between *Akkermansia muciniphila* and intestinal epithelium controls diet-induced obesity. *Proc. Natl. Acad. Sci. U.S.A.* **2013**, *110*, 9066−9071.
(46) Cani, T.; Gao, Y.; Hao, J.; Yin, J.; Li, W.; Geng, J.; Liu, R.; Sui, W.; Zhang, M. Lycopene, amaranth, and sorghum red pigments counteract

https://dx.doi.org/10.1021/acs.jafc.0c06426
J. Agric. Food Chem. 2021, 69, 198−211

obesity and modulate the gut microbiota in high-fat diet fed C57BL/6 mice. *J. Funct. Foods* **2019**, *60*, 103437.
(47) Zhang, L.; Shi, M.; Ji, J.; Hu, X.; Chen, F. Gut microbiota determines the prevention effects of Luffa cylindrica (L.) Roem supplementation against obesity and associated metabolic disorders induced by high-fat diet. *FASEB J.* **2019**, *33*, 10339−10352.
(48) Jiao, X.; Wang, Y.; Lin, Y.; Lang, Y.; Li, E.; Zhang, X.; Zhang, Q.; Feng, Y.; Meng, X.; Li, B. Blueberry polyphenols extract as a potential prebiotic with anti-obesity effects on C57BL/6 J mice by modulating the gut microbiota. *J. Nutr. Biochem.* **2019**, *64*, 88−100.
(49) Konikoff, T.; Gophna, U. Oscillospira: a Central, Enigmatic Component of the Human Gut Microbiota. *Trends Microbiol.* **2016**, *24*, 523−524.
(50) Qiu, M.; Huang, K.; Liu, Y.; Yang, Y.; Tang, H.; Liu, X.; Wang, C.; Chen, H.; Xiong, Y.; Zhang, J.; Yang, J. Modulation of intestinal microbiota by glycyrrhizic acid prevents high-fat diet-enhanced pre-metastatic niche formation and metastasis. *Mucosal Immunol.* **2019**, *12*, 945−957.
(51) Esposito, D.; Damsud, T.; Wilson, M.; Grace, M. H.; Strauch, R.; Li, X.; Lila, M. A.; Komarnytsky, S. Black Currant Anthocyanins Attenuate Weight Gain and Improve Glucose Metabolism in Diet-Induced Obese Mice with Intact, but Not Disrupted, Gut Microbiome. *J. Agric. Food Chem.* **2015**, *63*, 6172−6180.
(52) Zeng, S.-L.; Li, S.-Z.; Xiao, P.-T.; Cai, Y.-Y.; Chu, C.; Chen, B.-Z.; Li, P.; Li, J.; Liu, E.-H. Citrus polymethoxyflavones attenuate metabolic syndrome by regulating gut microbiome and amino acid metabolism. *Sci. Adv.* **2020**, *6*, No. eaax6208.
(53) Sekhon-Loodu, S.; Ziaullah; Rupasinghe, H. P. V. Docosahexaenoic acid ester of phloridzin inhibit lipopolysaccharide-induced inflammation in THP-1 differentiated macrophages. *Int. Immunopharmacol.* **2015**, *25*, 199−206.

https://dx.doi.org/10.1021/acs.jafc.0c06426
J. Agric. Food Chem. 2021, 69, 198−211